ADVANCED FUNCTIONAL MATERIALS
www.afm-journal.de

Materials Views
www.MaterialsViews.com

The Role of Transition Metal Oxides in Charge-Generation Layers for Stacked Organic Light-Emitting Diodes

By *Sami Hamwi, Jens Meyer, Michael Kröger, Thomas Winkler, Marco Witte, Thomas Riedl,* Antoine Kahn,* and *Wolfgang Kowalsky*

The mechanism of charge generation in transition metal oxide (TMO)-based charge-generation layers (CGL) used in stacked organic light-emitting diodes (OLEDs) is reported upon. An interconnecting unit between two vertically stacked OLEDs, consisting of an abrupt heterointerface between a Cs_2CO_3-doped 4,7-diphenyl-1,10-phenanthroline layer and a WO_3 film is investigated. Minimum thicknesses are determined for these layers to allow for simultaneous operation of both sub-OLEDs in the stacked device. Luminance–current density–voltage measurements, angular dependent spectral emission characteristics, and optical device simulations lead to minimum thicknesses of the n-type doped layer and the TMO layer of 5 and 2.5 nm, respectively. Using data on interface energetic determined by ultraviolet photoelectron and inverse photoemission spectroscopy, it is shown that the actual charge generation occurs between the WO_3 layer and its neighboring hole-transport material, 4,4',4''-tris(*N*-carbazolyl)-triphenyl amine. The role of the adjacent n-type doped electron transport layer is only to facilitate electron injection from the TMO into the adjacent sub-OLED.

1. Introduction

Organic light-emitting diodes (OLEDs) have attracted much interest in research and development in the last two decades. A long operating lifetime must be ensured before mass-production of OLEDs for the consumer market can start. An elegant way to meet this requirement using present organic materials and devices is to stack a number of OLEDs on top of each other, so as to significantly reduce the stress on each light-emitting unit while still achieving a given luminance level. Interconnecting units that serve as charge-generation layers (CGL) are required when driving OLED stacks as two-terminal devices. The first studies by Kido et al. suggested that indium tin oxide (ITO) or tetrafluorotetracyanoquinodimethane (F_4-TCNQ) adjacent to a hole-transport layer (HTL) may lead to the generation of holes and electrons upon application of an electric field.[1] Since this early work, various concepts for CGL structures have been published, including junctions between chemically p- and n-doped charge transport layer,[2–4] the insertion of thin metal or transparent conductive oxide (TCO) layers,[1,5] and the insertion of transition metal oxides (TMOs).[6–10]

It was recently shown that the charge-generation mechanism when using a doped organic p–n heterojunction is based on a temperature-independent field-induced charge separation supported by a large band bending at the interface. This interpretation was evidenced by results from Kelvin probe measurements.[11] On the other hand, speculation remains about the mechanism operating at TMO-based CGLs. Terai et al. proposed a thermal stimulation model in which the charge generation is claimed to be thermally assisted. Based on the assumption of impurity levels within the bandgap of V_2O_5, electrons are supposed to diffuse from the valence band of the TMO to the lowest unoccupied molecular orbital (LUMO) of the adjacent n-type doped electron-transport layer (ETL), which is regarded as the charge-generation mechanism.[12] Very recently, Qi et al. suggested a specific energy-level alignment between lithium-doped 4,7-diphenyl-1,10-phenanthroline (BCP) and MoO_3 to explain the charge-generation mechanism. The assumption made is that of a thermally assisted tunneling injection of electrons into the ETL and a concomitant hole generation within the TMO layer.[13] In that model, MoO_3 is assumed to be a p-type semiconductor with the valence band and conduction band located at 5.7 and 2.3 eV below vacuum level (E_{vac}), respectively. However, in view of recent reports on the electronics structure of MoO_3 this model must be revised.[14–17] Based on results obtained by ultraviolet and inverse photoemission

[*] Prof. T. Riedl
Institute of Electronic Devices
University of Wuppertal
Rainer-Gruenter-Str. 21
D-42119 Wuppertal (Germany)
E-mail: t.riedl@uni-wuppertal.de
S. Hamwi, T. Winkler, M. Witte, Prof. W. Kowalsky
Technical University of Braunschweig
Institute of High-Frequency Technology
Schleinitzstraße 22
D-38106 Braunschweig (Germany)
Dr. J. Meyer, Prof. A. Kahn
Department of Electrical Engineering
Princeton University
Princeton, NJ 08544 (USA)
Dr. M. Kröger
InnovationLab GmbH
Speyerer Straße 4
D-69115 Heidelberg (Germany)

DOI: 10.1002/adfm.201000301

spectroscopy (UPS and IPES), MoO_3 exhibits a deep lying conduction band at 6.7 eV and a high work function of 6.9 eV and therefore shows properties of an n-type semiconductor.[14] Similar results have been reported for other TMOs like WO_3 exhibiting a similarly high work function, first measured by Meyer et al. via Kelvin probe technique and confirmed by photoemission spectroscopy.[17,18] Consequently, the CGL model mentioned above, in which holes are claimed to be generated within the TMO and subsequently drift towards the HTL, must be revised entirely.

To clarify the TMO-based CGL mechanism, we present a detailed study of the interconnecting unit placed in a stacked double OLED structure. By conventional vertical stacking, an abrupt heterointerface is automatically formed between a Cs_2CO_3-doped 4,7-diphenyl-1,10-phenanthroline (BPhen) layer as the topmost ETL of the bottom light-emitting unit, and WO_3 as the lowermost constituent of the top OLED (Fig. 1). To analyze the functionality of the interconnecting unit, we vary the thickness of its components and measure the electro-optical properties of the stacked OLEDs. With the help of luminance–current density–voltage (*L–I–V*) measurements, the analysis of the angular resolved spectral emission characteristics, and simultaneous optical device simulation, we unambiguously identify the minimum required thickness that makes each individual constituents of the interconnecting unit fully functional. Using the energetics determined via UPS and IPES for the interfaces between the interconnecting unit and adjacent charge transport layers,[19] we demonstrate that the actual charge generation process takes place at the interface between the thin film of WO_3 and the neighboring HTL. A large interface dipole between these two layers is found. These results prove former assumptions of a thermally assisted charge-generation mechanism within the TMO to be invalid. Based on these findings, we suggest a general design rule for CGLs involving TMOs.

2. Results and Discussion

The twofold stacked OLEDs were prepared by stacking two green light-emitting organic diodes with identical layer sequence on-top of each other (Fig. 1). Each OLED comprises a thin film of WO_3 followed by 4,4',4''-tris(*N*-carbazolyl)-triphenyl amine (TCTA) as the HTL and 1,3,5-tris(phenyl-2-benzimidazolyl)-benzene (TPBi) as the ETL. The emission layer is formed by fac tris (2-phenylpyridine)iridium ($Ir(ppy)_3$)-doped TPBi (7 vol%) located between the HTL and the ETL. Finally, each OLED unit is capped by Cs_2CO_3-doped BPhen (16 wt%) as an efficient electron-injecting layer (EIL). Indium tin oxide (ITO) and Al are used as bottom and top electrode, respectively.

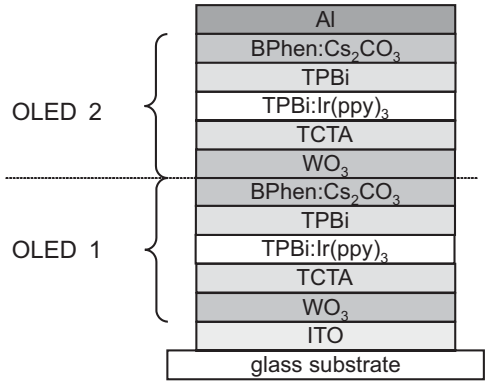

Figure 1. Layer sequence of the twofold stacked OLED.

2.1. Critical Layer Thickness

As a first step to study the heterointerface between both sub-OLEDs, we varied the thickness of the WO_3 layer in OLED 2 (Fig. 1) from 0 to 5 nm and simultaneously changed the thickness of the neighboring HTL from 45 to 40 nm, keeping the overall thickness of the stacked OLEDs as well as the distance between the emission layers and the electrodes constant (Table 1, series A). The current efficiency (η) versus luminance (L) characteristics are shown in Fig. 2a. Without WO_3, or for a TMO thickness less than 1.5 nm, the stacked OLEDs only exhibit low current efficiencies of about 10 cd A^{-1}. This changes abruptly for a thickness of the TMO layer of 2.5 nm and beyond, for which the current efficiencies jump to values between 50 and 56 cd A^{-1} (at 1 000 cd m^{-2}). Furthermore, we observed that only for devices with WO_3 layer thickness larger than 2 nm the onset voltage is less than 5 V (not shown here). This indicates an efficient charge-generation mechanism, since the onset voltage is only twice that of each individual sub-OLED of similar structure.[18] In this case, no significant potential drop occurs within the CGL to generate and separate the charge carriers. The first result of this experiment is therefore that the CGL interconnecting architecture is not fully functional in stacked OLED devices as long as the WO_3 layer thickness is below some critical value. A further set of experiments leads to a similar conclusion regarding the EIL, in that the efficiency of stacked OLEDs is significantly lower than 60 cd A^{-1} when using insufficiently thick films of Cs_2CO_3-doped BPhen at the CGL heterointerface. The thickness of the n-doped ETL of OLED 1 (Fig. 1) is varied from 0 to 10 nm while simultaneously changing the thickness of the neighboring layer of TPBi from 50 to 40 nm and keeping the thickness of WO_3 at 5 nm as well as the overall thickness of the stacked OLEDs constant (Table 1, series B). Starting at a doped BPhen thickness below 5 nm, we obtained a current efficiency around 40 cd A^{-1} (Fig. 2b). As the layer thickness increases to 5 nm and beyond, the current efficiency again jumps to higher values of around 55 to 60 cd A^{-1}, indicating full functionality of the stacked device.

Table 1. Layer sequence and thicknesses (given in nm) of the two OLED series A and B.

	Layer	Series A	Series B
		Al top electrode	
OLED 2	BPhen:Cs_2CO_3	20	20
	TPBi	30	30
	TPBi:$Ir(ppy)_3$	10	10
	TCTA	(45 – X)	40
	WO_3	X	5
OLED 1	BPhen:Cs_2CO_3	20	Y
	TPBi	30	(50 – Y)
	TPBi:$Ir(ppy)_3$	10	10
	TCTA	40	40
	WO_3	5	5
		ITO bottom electrode	

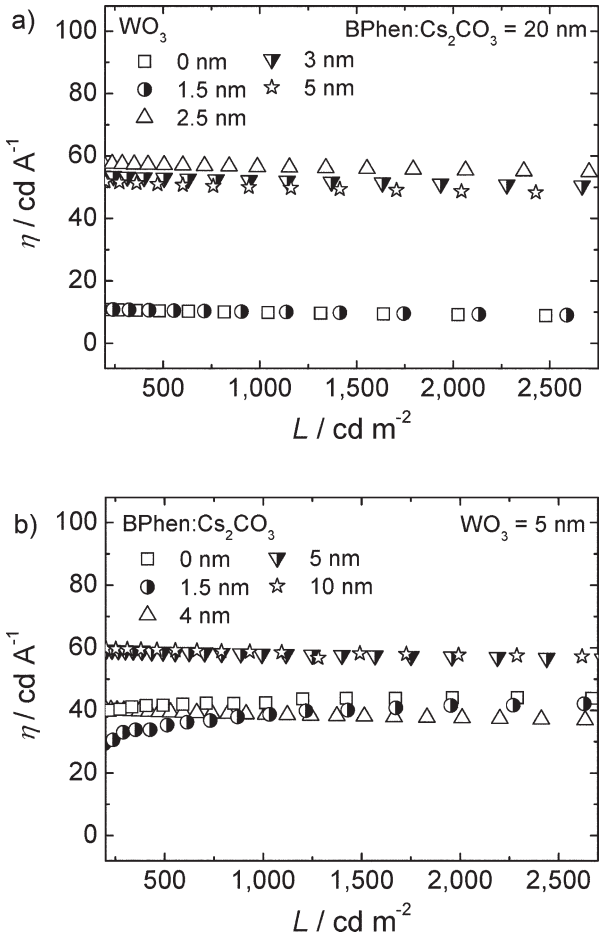

Figure 2. η versus L characteristics of the twofold stacked OLEDs upon a) variation of the WO_3 layer thickness with constant thickness of the BPhen:Cs_2CO_3 component (series A) and b) variation of BPhen:Cs_2CO_3 thickness with constant thickness of WO_3 (series B).

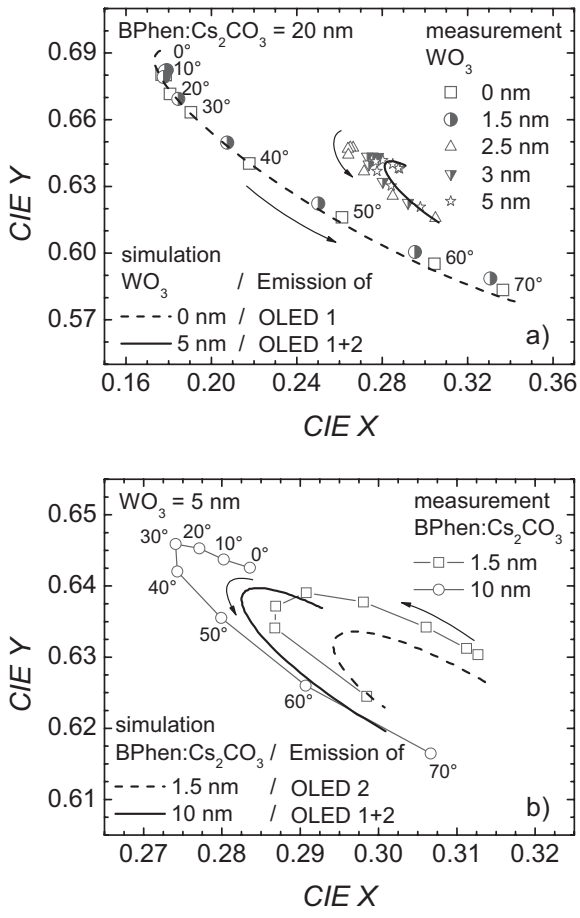

Figure 3. CIE characteristics of angular resolved EL spectra obtained by measurement and optical device simulation for a) series A and b) series B.

To clarify the nature of an incomplete interconnecting unit and its impact on the operation of the stacked OLEDs, we conducted angular-dependent measurements of the electroluminescence (EL) spectra and compared the results with optical device simulation. For a better illustration, the EL spectra are converted to CIE (Commission Internationale de l'Eclairage) coordinates and summarized within respective sections of the CIE color space diagrams (Fig. 3). While the stacked OLEDs with a WO_3 layer below the critical thickness showed highly angular-dependent CIE characteristics, the situation changed with increased thickness of the TMO layer (Fig. 3a). There, the CIE values only ranged from $X = 0.64$ to 0.62 and from $Y = 0.28$ to 0.30 for angles between 0° and 70°. The same characteristics are obtained with optical device simulation by assuming full operation of both light-emitting units. However, in case of stacked OLEDs with an incomplete heterointerface (with WO_3 thickness below 2 nm), the CIE characteristics can only be reproduced if we assume that only OLED 1 emits light. As a result it is essential to note, that the low efficiency of the entire stack cannot be explained by two partially functional sub-OLEDs. On the other hand, this result indicates that the contribution of sub-OLED 1 to the total current efficiency is less than that of sub-OLED 2 operated under similar conditions, as reflected by the L–I–V measurements above (Fig. 2a). Thereby, the asymmetric contribution of both light-emitting units to the luminance must be attributed to the non-optimal distance of the emission layer of sub-OLED 1 to the metallic top contact, which leads to a substantially lower out-coupling efficiency for this light-emitting unit. Similarly, the comparison between experiment and simulation upon variation of the thickness of the Cs_2CO_3-doped BPhen film demonstrates the following. Full operation of both light-emitting units is achieved for thick layers of BPhen:Cs_2CO_3, whereas light emission from only sub-OLED 2 is obtained for a BPhen:Cs_2CO_3 thickness below 5 nm (illustrated by two CIE characteristics in Fig. 3b). As a first result of these electro-optical studies, we conclude that 5 nm of n-type doped BPhen and 2.5 nm of WO_3 represent the critical thicknesses for full operation of both sub-OLEDs of the entire stacked device. When only one sub-OLED is actually emitting, a leakage current through the non-emitting sub-OLED must supply charge carriers for the emitting sub-OLED, leading to comparatively high operating voltages for these stacked OLEDs (not shown here).

2.2. CGL: Principle of Operation

All reports on CGL units published so far emphasize the requirement of an n-type doped organic semiconductor layer

adjacent to a p-type doped layer, a TCO layer, or a TMO layer. This is strong evidence of the essential role played by such a layer in the mechanisms operating in the CGL. In the following, we show that it serves as EIL, while the actual process of charge generation occurs at a different interface. We use the electronic structure of the interface between Cs_2CO_3-doped BPhen and WO_3 determined via UPS and IPES.[19] As shown in previous Kelvin probe and UPS measurements, a 10-nm-thick layer of WO_3 (deposited on Au-coated n+ doped Si) exhibits a high work function (WF) of 6.68 eV.[17,18] The electron affinity (EA) and ionization energy (IE) of such a layer have been found equal to 6.45 and 9.83 eV via IPES and UPS measurements, respectively. The small energy difference between EA and WF indicates that the Fermi level E_F is very close to the TMO conduction band minimum and thus that the TMO is a highly n-type doped semiconductor, presumably due to oxygen vacancy defects acting as donors in transparent conducting oxides.[20] For MoO_3, the formation of oxygen deficient films has been evidenced by X-ray photoelectron spectroscopy and is attributed to the decomposition and preferential evaporation of the lower vapor pressure constituent atomic species.[21,22]

During the gradual deposition of Cs_2CO_3-doped BPhen (9 wt%) onto WO_3, the WF Φ of the film decreases with almost parabolic characteristics, indicating the formation of a space charge region within the organic ETL (Fig. 4). Starting with the large value corresponding to the neat layer of WO_3, Φ drops and finally saturates at 2.5 eV for thicknesses d of 13–26 nm. The saturation actually occurs at approximately 7.5 nm when considering the parabolic characteristics of the work function indicated by the fit (Fig. 4). Taking into account the IE (6.8 eV) and EA (2.4 eV) of BPhen:Cs_2CO_3 measured by UPS and IPES, the energy level alignment at the interface with the TMO can be represented as shown in Figure 5, which corresponds to the heterointerface between the bottom OLED 1 and the top OLED 2. It is evident from this schematic that no charge generation occurs between the n-type doped BPhen and the TMO layer. On the other hand, electrons reaching this interface can tunnel from the conduction band (CB) of WO_3 through the narrow potential barrier into the LUMO of the n-doped organic ETL. The higher tunneling probability is strongly supported by the fact that the high WF difference of the TMO and BPhen:Cs_2CO_3 amounts to 4.2 eV, leading to iso-energetic electron levels in the CB of WO_3 and LUMO of the ETL. These results also explain that below the minimum thickness of n-type doped BPhen

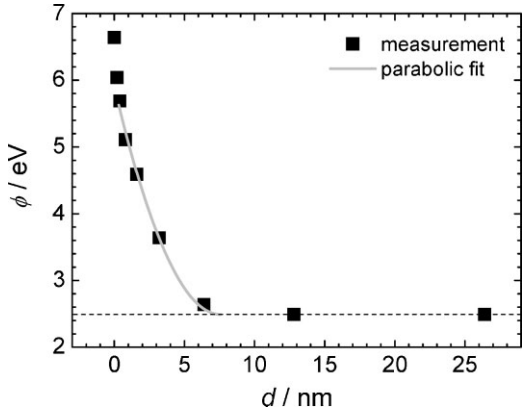

Figure 4. Φ measured by UPS on Cs_2CO_3-doped BPhen (9 wt%) with thickness d deposited on 10 nm of WO_3.

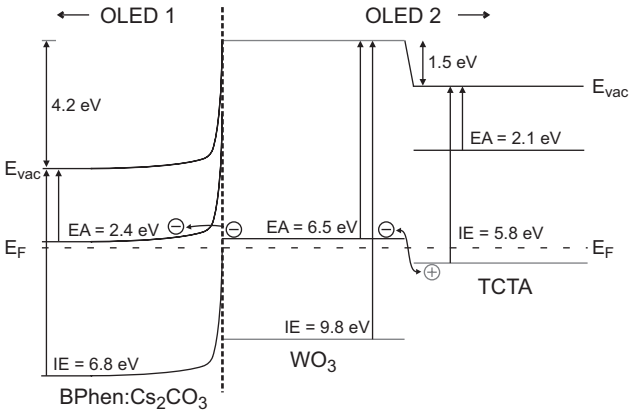

Figure 5. Energy level diagram of the BPhen:Cs_2CO_3/WO_3/TCTA junction determined by UPS and IPES (spectra of these measurements will be published elsewhere) [19].

layer, an incomplete space charge region forms, the WF does not reach saturation in the BPhen-covered WO_3, and the built-in potential remains too low to allow for efficient tunneling of electrons. In that case, the energy difference between the CB of WO_3 and the LUMO of BPhen:Cs_2CO_3 increases as the thickness of the n-type doped layer decreases. Concomitantly, the shape of the tunnel barrier for electrons changes unfavorably into a rectangle. Taking into account the fact that the n-type doping concentration used in the stacked OLEDs was higher than in the samples studied by UPS/IPES, the minimum thickness of 5 nm found above is in favorable agreement with the characteristic width of the space charge region derived here. On the other hand, the 2.5-nm minimum thickness of WO_3 found in our electro-optical studies is believed to be simply related to the required amount of deposited material necessary to form a continuous layer of TMO. From the study of the heterointerface between the stacked OLEDs, we can unambiguously conclude that the Cs_2CO_3-doped BPhen only acts as an EIL and is not directly involved in the charge-generation process. Consequently, the actual charge-generation mechanism must be attributed to the heterointerface between WO_3 and TCTA within OLED 2. UPS and IPES measurements show an interfacial dipole $\Delta = 1.5$ eV between the two materials, complete with only 1.6 nm of the organic material, as well as a small (0.8 eV) barrier between the highest occupied molecular orbital (HOMO) of TCTA and the CB of WO_3.[19] This electronic configuration allows therefore electrons to be injected into the TMO CB, resulting in a hole in the HTL. Note that this interface molecular level alignment is entirely equivalent to that recently found by Kröger et al. for interfaces between MoO_3 or WO_3 and another HTL, *N,N'*-diphenyl-*N,N'*-bis(1-naphthyl)-1,1'-biphenyl-4,4'-diamine (α-NPD).[16,23]

Accordingly, our findings cast some doubt on the recently published hypothesis about a two-step process of a charge generation directly within the TMO and an electron injection afterwards based on a tunneling-assisted thermionic emission into the n-type doped ETL, since that explanation neglects recent results concerning the electronic structure of TMOs.[13] The resulting misconception denotes the combination of n-type doped ETL and TMO as the essential components of a CGL. According to our study, the combination of the TMO and HTL films can be regarded as the actual CGL, given the high work function and the deep lying

CB of the TMOs on the one hand, and the energy level alignment with the HOMO of the adjacent HTL on the other. This result appears to be of general nature, as the recent results reported by Kröger et al. show that the hole injection from MoO_3 into α-NPD is based on a similar mechanism.[16] It is also worth noting that the role of TMOs in CGLs can be compared with the one of, for example, 1,4,5,8,9,11-hexaazatriphenylene-hexacarbonitrile (HAT-CN), which also exhibits a high WF (~6 eV) and a deep lying LUMO level. This leads to the same electric-field-assisted charge-generation mechanism at the interface between HAT-CN and a hole transport material.[24,25] As a consequence, the n-type doped BPhen is only required to enable an efficient electron injection from the TMO into the bottom OLED unit. The formation of an interfacial dipole is also likely at the interface between TMO and a non-doped ETL. This could possibly explain the steep decay of the WF within the first few monolayers of BPhen:Cs_2CO_3 deposited on top of the TMO, leading to some local deviation from the ideal parabolic fit (Fig. 4, first few nanometers). However, the value of the dipole is supposed to amount between 1.5 and 2 eV, which is not sufficient for an electron injection from the deep lying CB of the TMO into the LUMO of a non-doped ETL like TPBi as has been shown by our electro-optical studies.

3. Conclusions

In summary, we have demonstrated that the charge-generation mechanism in TMO-based interconnecting units of stacked OLEDs occurs at the heterointerface between the TMO and the adjacent non-doped hole-transporting layer (e.g., TCTA). Despite a substantial interfacial dipole of 1.5 eV, the energetic difference between the CB of WO_3 and the HOMO of TCTA only amounts to 0.8 eV, allowing for an efficient charge generation and separation at this interface. Consequently, the combination of TMO and HTL states the actual CGL. This is due to the nature of TMOs like WO_3 and MoO_3 having a deep-lying conduction band and a high WF. Accordingly, an electric-field-assisted charge-generation process takes place. Consequently, the adjacent n-type doped electron transport layer is only used to facilitate the electron injection from the TMO into the adjacent sub-OLED. These results have been used to explain the experimental results on twofold stacked OLEDs with a corresponding CGL architecture. In order to find both sub-OLEDs fully functional, a critical thickness of the doped ETL and the TMO has been determined to be 5 and 2.5 nm, respectively.

4. Experimental

The device preparation and characterization was carried out at the TU Braunschweig. All devices were prepared on commercial glass substrates coated with 140-nm-thick ITO with a sheet resistance of 14 $\Omega\,sq^{-1}$ (Merck). The deposition of the organic and inorganic films were carried out by thermal evaporation within a 10^{-8} mbar vacuum system with separate deposition chambers for n-type doping as well as transport and emitting materials and metal contact. The deposition rate for all organic and inorganic materials was controlled by quartz-crystal monitors and kept constant within the range from 0.02 to 0.1 nm s^{-1}. For the evaporation of WO_3 and Cs_2CO_3 we used shielded high-temperature evaporation sources (CreaTec). The doping of TPBi and BPhen with $Ir(ppy)_3$ and Cs_2CO_3, respectively, was made by thermal co-evaporation controlled via two separate quartz-crystal monitors. A Keithley 2400 source meter in combination with a calibrated Advantest TQ 8221 photodetecting unit was applied for *L–I–V* measurements under ambient conditions. The angular resolved EL spectra were obtained by an optical fiber connected with an imaging monochromator system (Triax320, CCD4000, Jobin Yvon). Thereby, the stacked OLEDs were operated at current densities from 10 to 80 mA cm^{-2}. The maximum angle of collection given by the measurement setup can be estimated to 0.1°. Optical device simulation was performed by the commercial software ETFOS (Fluxim). The optical parameters of the organic materials in the device stack have been obtained by spectroscopic ellipsometry (Sopra). The UPS and IPES measurements were conducted at Princeton University. Details of the experimental setup are given elsewhere [19].

Acknowledgements

Work in Braunschweig was financially supported by the German Federal Ministry for Education and Research (FKZ: 13N8995, 13N9152). Work in Princeton was supported by the National Science Foundation (Grant No. DMR-0705920) and the Princeton MRSEC of the NSF (Grant No. DMR-0819860). J. M. thanks the Deutsche Forschungsgemeinschaft (DFG) for generous support within the postdoctoral fellowship program.

Received: February 12, 2010
Published online: May 14, 2010

[1] J. Kido, T. Matsumoto, T. Nakada, J. Endo, K. Mori, N. Kawamura, A. Yokoi, *SID Int. Symp. Dig. Tech. Pap.* **2003**, *34*, 979.
[2] L. S. Liao, K. P. Klubek, C. W. Tang, *Appl. Phys. Lett.* **2004**, *84*, 167.
[3] T.-Y. Cho, C.-L. Lin, C.-C. Wu, *Appl. Phys. Lett.* **2006**, *88*, 111106.
[4] X. D. Gao, J. Zhou, Z. T. Xie, B. F. Ding, Y. C. Qian, X. M. Ding, X. Y. Hou, *Appl. Phys. Lett.* **2008**, *93*, 083304.
[5] J. X. Sun, X. L. Zhu, H. J. Peng, M. Wong, H. S. Kwok, *Appl. Phys. Lett.* **2005**, *87*, 093504.
[6] F. Guo, D. Ma, *Appl. Phys. Lett.* **2005**, *87*, 173510.
[7] C.-W. Chen, Y.-J. Lu, C.-C. Wu, E. H.-E. Wu, C.-W. Chu, Y. Yang, *Appl. Phys. Lett.* **2005**, *87*, 241121.
[8] C.-C. Chang, J.-F. Chen, S.-W. Hwang, C. H. Chen, *Appl. Phys. Lett.* **2005**, *87*, 253501.
[9] H. Kanno, R. J. Holmes, Y. Sun, S. Kena-Cohen, S. R. Forrest, *Adv. Mater.* **2006**, *18*, 339.
[10] D.-S. Leem, J.-H. Lee, J.-J. Kim, J.-W. Kang, *Appl. Phys. Lett.* **2008**, *87*, 103304.
[11] M. Kröger, S. Hamwi, J. Meyer, T. Dobbertin, T. Riedl, W. Kowalsky, H.-H. Johannes, *Phys. Rev. B* **2007**, *75*, 235321.
[12] M. Terai, K. Fujita, T. Tsutsui, *Jpn. J. Appl. Phys* **2005**, *44*, L 1059.
[13] X. Qi, N. Li, S. R. Forrest, *J. Appl. Phys.* **2010**, *107*, 014514.
[14] M. Kröger, S. Hamwi, J. Meyer, T. Riedl, W. Kowalsky, A. Kahn, *Org. Electron.* **2009**, *10*, 932.
[15] D. Y. Kim, J. Subbiah, G. Sarasqueta, F. So, H. Ding, Irfan, Y. Gao, *Appl. Phys. Lett.* **2009**, *95*, 093304.
[16] K. Kanai, K. Koizumi, S. Ouchi, Y. Tsakamoto, K. Sakanoue, Y. Ouchi, K. Seki, *Org. Electron.* **2010**, *11*, 188.
[17] M. Kröger, S. Hamwi, J. Meyer, T. Riedl, W. Kowalsky, A. Kahn, *Appl. Phys. Lett.* **2009**, *95*, 123301.
[18] J. Meyer, S. Hamwi, T. Bülow, H.-H. Johannes, T. Riedl, W. Kowalsky, *Appl. Phys. Lett.* **2007**, *91*, 113506.
[19] J. Meyer, M. Kröger, S. Hamwi, T. Riedl, W. Kowalsky, A. Kahn, unpublished.
[20] S. Samson, C. G. Fonstad, *J. Appl. Phys* **1973**, *44*, 4618.
[21] T. S. Sian, G. B. Reddy, *Sol. Energy Mater. Sol. Cells* **2004**, *82*, 375.
[22] K. S. Rao, K. V. Madhuri, S. Uthanna, O. M. Hussain, C. Julien, *Mat. Sci. Eng. B* **2003**, *100*, 79.
[23] J. Meyer, A. Shu, M. Kröger, A. Kahn, *Appl. Phys. Lett.* **2010**, *96*, 133308.
[24] L. S. Liao, K. P. Klubek, *Appl. Phys. Lett.* **2008**, *92*, 223311.
[25] Y.-K. Kim, J. W. Kim, Y. Park, *Appl. Phys. Lett.* **2009**, *94*, 063305.